*Organometallics* **2003,** *22,* 3077−3082

# Theoretical Study of Coordination and Insertion of Butadiene to Bis(pentamethylcyclopentadienyl)samarium Hydride

Shojiro Kaita,[†,‡] Nobuaki Koga,[§] Zhaomin Hou,[‡] Yoshiharu Doi,[‡] and Yasuo Wakatsuki*,[†]

*OM Chem-Tech Co. Ltd., Cooperation Center Building, Hirosawa 2-1, Wako, Saitama 351-0198, Japan, RIKEN, Hirosawa 2-1, Wako, Saitama 351-0198, Japan, and Graduate School of Information Science, Nagoya University, Nagoya 464-8601, Japan*

*Received March 5, 2003*

The precise mechanism of the reaction of butadiene with $Cp^*_2Sm(H)$ ($Cp^* = \eta^5$-$C_5Me_5$) has been investigated on the basis of DFT calculations. The initial coordination of butadiene to the $Cp^*_2Sm(H)$ moiety was found to be $\eta^2$-fashion, $\eta^4$-coordination being sterically difficult. The experimentally known insertion product, $Cp^*_2Sm(\eta^3$-$CH_2CHCHMe)$ (**1a**), where the methyl group is in the *syn* position, is thermodynamically more stable than the *anti*-isomer (**1c**) by 5.7 kcal/mol. The *anti* → *syn* transformation, i.e., isomerization of **1c** to **1a**, is possible via an intermediate with an $\eta^1$-$CH(Me)CH{=}CH_2$ ligand but requires a rather high energy barrier of 22 kcal/mol. Rotational motion of the allylic ligand in **1a** takes place through a [Sm-$\eta^1$-$CH_2CH{=}CHMe$] intermediate, i.e., through another $\eta^3 \rightarrow \eta^1$ change of the allylic coordination or dissociation of the double bond. Complex **1a** can be formed directly by the insertion of an $\eta^2$-coordinated *trans*-butadiene to the Sm−H bond through an early transition state with very small activation energy. In contrast, **1c** is derived from a complex with an $\eta^2$-coordinated *cis*-butadiene via an $\eta^1$-butenyl intermediate complex. The *syn*-configurated $\eta^3$-butenyl complex **1a** is thus the most preferred product in terms of both kinetics and thermodynamics.

## Introduction

The reaction of samarocene hydride $(Cp^*_2SmH)_2$ ($Cp^* = \eta^5$-$C_5Me_5$) with butadiene has been known to give $Cp^*_2Sm(\eta^3$-$CH_2CHCHMe)$ (**1a**), and its solid-state structure determined by X-ray analysis has proved that the butenyl unit adopts a *syn*-form.[1] A similar reaction is known also for $(Cp^*_2LaH)_2$.[2] We are interested in this seemingly simple insertion reaction because it could be a primitive model relevant to the recently found highly *cis*-regulated 1,4-polymerization of butadiene catalyzed by $Cp^*_2Ln(Me)$ (Ln = Sm, Nd, Gd) or related complexes in the presence of cocatalysts such as MAO.[3] The true active species for this polymerization is not known yet because the presence of cocatalyst makes the system complicated. Although complexes such as **1a** have been reported to be inactive for polymerization of butadiene when used alone,[2] it appeared important to clarify the behavior of a butadiene molecule in the coordination sphere of $Cp^*_2Ln(R)$ (R = H or alkyl), because it could give potential clues to speculate the role of cocatalysts in the above-mentioned polymerization catalysis. Furthermore, an $\eta^3$ to $\eta^1$ change in coordination of the butenyl ligand in **1a** and concomitant *syn* ⇄ *anti* interconversion is of interest as a factor to be considered when elucidating the origin of stereospecificity of butadiene polymerization catalyzed by this and related systems.[4]

Compared to a large number of theoretical studies on insertion reactions of olefins into metal−hydrogen or metal−carbon bonds of d-block transition metals, only a few theoretical papers have treated such reactions involving lanthanide metals. Koga recently reported ab initio calculations on insertion of ethylene into the the metal−H or metal−C bond of $Cp_2Sm(R)$ ($Cp = \eta^5$-$C_5H_5$, R = H, Me).[5] The reaction was analyzed to proceed via a rather straightforward four-centered transition state similar to those found in the corresponding reactions of d-block metals, e.g., $[Cp_2Ti(R)]^+$. The computed activation energy for the insertion of ethylene to Sm−H was quite small, 4.2 kcal/mol by MP4SDQ/MP2 level calculations. However, when butadiene is substituted for ethylene, the same reaction could be much more complicated due to the presence of an additional conjugated vinyl group as well as its larger steric bulk. To take into account the steric factors, we describe in this

---

* Corresponding author. Tel/Fax: +81-48-468-5063. E-mail: waky@postman.riken.go.jp.

[†] OM Chem-Tech.

[‡] RIKEN.

[§] Nagoya University.

(1) Evans, W. J.; Ulibarri, T. A.; Ziller, J. W. *J. Am. Chem. Soc.* **1990**, *112*, 2314.

(2) Jeske, G.; Lauke, H.; Mauermann, H.; Swepston, P. N.; Schumann, H.; Marks, T. J. *J. Am. Chem. Soc.* **1985**, *107*, 8091.

(3) (a) Kaita, S.; Hou, Z.; Wakatsuki, Y. *Macromolecules* **1999**, *32*, 9078. (b) Kaita, S.; Hou, Z.; Wakatsuki, Y. *Macromolecules* **2001**, *34*, 1539. (c) Hou, Z.; Kaita, S.; Wakatsuki, Y. *Pure Appl. Chem.* **2001**, *73*, 291. (d) Kaita, S.; Hou, Z.; Nishiura, M.; Doi, Y.; Kurazumi, J.; Horiuchi, A. C.; Wakatsuki, Y. *Macromol. Rapid Commun.* **2003**, *24*, 179.

(4) Tobisch, S. *Acc. Chem. Res.* **2002**, *35*, 96.

(5) (a) Koga, N. *Theor. Chem. Acc.* **1999**, *102*, 285. (b) Kulkarni, S. A.; Koga, N. *J. Mol. Struct. (THEOCHEM)* **1999**, *461−462*, 297.

10.1021/om030162e CCC: $25.00

paper rather large realistic metal complexes with Cp*-based spectator ligands rather than adopting a simplified Cp-based model with a more sophisticated and reliable computaional approach.

## Computational Details

Since 4f orbitals are much smaller than 6s and 5d orbitals, it is generally accepted that 4f orbitals are not responsible for chemical bonds of lanthanide metal complexes. For Sm, we therefore adopted the relativistic effective core potential (ECP) developed by Dolg et al. together with (7s6p5d)/[5s4p3d] valence basis functions.[6] This ECP treats [Kr]$4d^{10}4f^5$ as a fixed core, whereas $5s^25p^66s^25d^16p^0$ shells are explicitly taken into consideration. Moreover, the ECP of this type was successfully used in the calculations of divalent lanthanide metallocenes[7a] and analysis of the reaction of trivalent $Cp_2LnH$ with $H_2$.[7b]

Preliminary geometry optimizations of stationary points were performed by the restricted Hartree−Fock (RHF) calculations using the Gaussian 98 program[8] with the 6-31G* basis set[9] for all C and H atoms. All of the obtained structures and energies were further refined by geometry optimizations based on B3LYP hybrid density functional methods with the 6-31G* basis set for the reacting ligands (hydride and butadiene) and the 6-31G basis set[10] for the two Cp* ligands. All transition states were checked by frequency calculations to prove that they were saddle points of order 1: the values of imaginary frequencies are provided as Supporting Information. Furthermore, all the transition states were relaxed to confirm that they do indeed connect the corresponding reactants and products.

## Results and Discussion

**(1) Comparison of an Observed and Computed Structure.** Two of the complexes relevant to the present study, $Cp^*_2Sm(\eta^3\text{-butenyl})$ (**1a**) and $Cp^*_2Sm(\eta^3\text{-allyl})$, have been prepared and structurally characterized by Evans et al.[1] To assess the present computational method, the computed geometry for **1a** and the corresponding bond parameters observed in the solid state are compared in Figure 1. In addition, the Sm−C(allyl) distances found in $Cp^*_2Sm(\eta^3\text{-allyl})$ are 2.630(15) and 2.643(18) Å for the terminal carbons and 2.668(18) Å for the central carbon. Though the calculated Sm−C distances tend to be longer than those of the observed values in crystals, the differences in important bond lengths are within 0.1 Å and well acceptable considering the size of the molecule and rather large standard deviations of the crystal analysis. Ab initio calculations by Dolg et al. on lanthanide metallocenes $Cp_2Ln$ (Ln = Sm, Eu, Yb) also resulted in longer M−C distances as compared to their X-ray analysis by 0.14−0.17 Å with RHF calculations and 0.07−0.09 Å with MP2 calculations.[7a] It has been pointed out that strongly correlated wave functions with adequately large basis set and inclusion of higher excitations would be necessary to obtain accurate metal−ligand distances in lanthanide metallocenes.

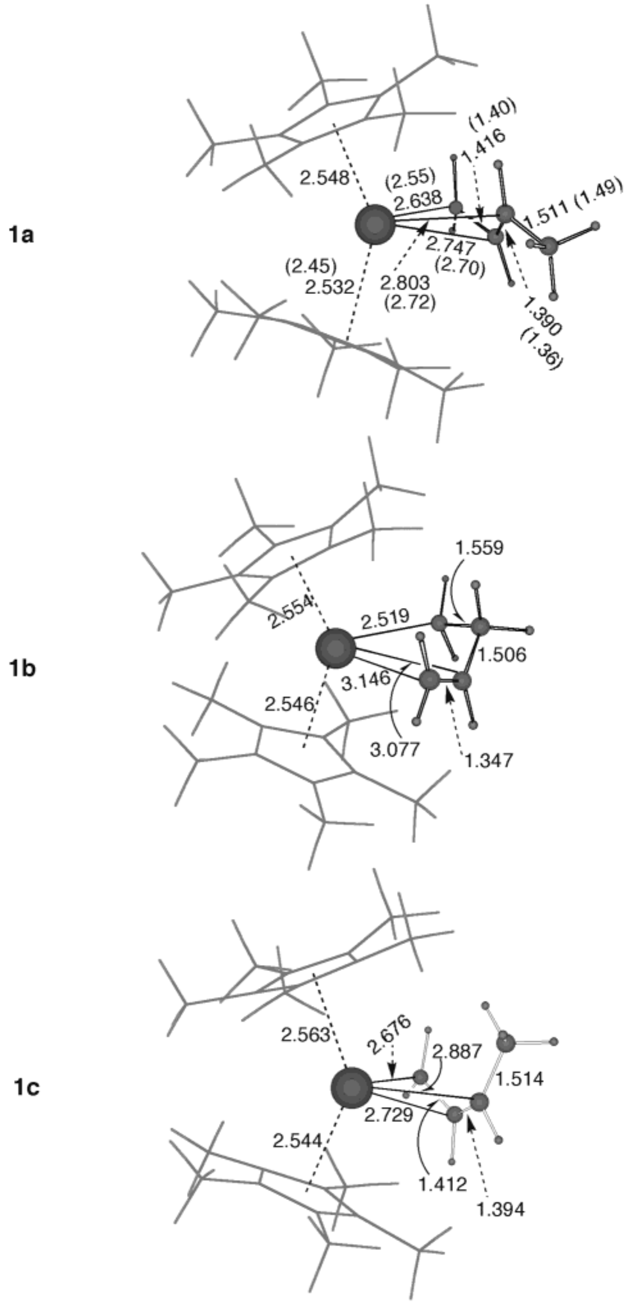

**Figure 1.** Computed structures (Å) of complexes with an $\eta^3$-coordinated butenyl group: **1a**, *syn*-allylic coordination (the X-ray structure in parentheses); **1b**, but-1-ene-4-yl coordination; **1c**, *anti*-allylic coordination.

**(2) Isomers of the $\eta^3$-Butenyl Complex.** Two isomers of **1a** are conceivable, and their computed structures viewed from the side are compared in Figure 1. Complex **1c** is the corresponding *anti*-$\pi$-allylic isomer, whereas **1b** has a nonconjugative but-1-ene-4-yl ligand. Also, their top view images are shown in Chart 1: in the present report, top views of all the complexes are

---

[6] Dolg, M.; Stoll, A.; Preuss, H. *Theor. Chim. Acta*, **1988**, *75*, 173.

[7] (a) Kaupp, M.; Schleyer, P. v. R.; Dolg, M.; Stoll, H. *J. Am. Chem. Soc.* **1992**, *114*, 8202. (b) Maron, L.; Eisenstein, O. *J. Am. Chem. Soc.* **2001**, *123*, 1036.

[8] Frisch, M. J.; Trucks, G. W.; Schlegel, H. B.; Scuseria, G. E.; Robb, M. A.; Cheeseman, J. R.; Zakrzewski, V. G.; Montgomery, J. A., Jr.; Stratmann, R. E.; Burant, J. C.; Dapprich, S.; Millam, J. M.; Daniels, A. D.; Kudin, K. N.; Strain, M. C.; Farkas, O.; Tomasi, J.; Barone, V.; Cossi, M.; Cammi, R.; Mennucci, B.; Pomelli, C.; Adamo, C.; Clifford, S.; Ochterski, J.; Petersson, G. A.; Ayala, P. Y.; Cui, Q.; Morokuma, K.; Malick, D. K.; Rabuck, A. D.; Raghavachari, K.; Foresman, J. B.; Cioslowski, J.; Ortiz, J. V.; Baboul, A. G.; Stefanov, B. B.; Liu, G.; Liashenko, A.; Piskorz, P.; Komaromi, I.; Gomperts, R.; Martin, R. L.; Fox, D. J.; Keith, T.; Al-Laham, M. A.; Peng, C. Y.; Nanayakkara, A.; Challacombe, M.; Gill, P. M. W.; Johnson, B.; Chen, W.; Wong, M. W.; Andres, J. L.; Gonzalez, C.; Head-Gordon, M.; Replogle, E. S.; Pople, J. A. *Gaussian 98*; Gaussian, Inc.: Pittsburgh, PA, 1998.

[9] Petersson, G. A.; Al-Laham, M. A. *J. Chem. Phys.* **1991**, *94*, 6081.

[10] Binning, R. C., Jr.; Curtiss, L. A. *J. Comput. Chem.* **1990**, *11*, 1206.

**Chart 1**

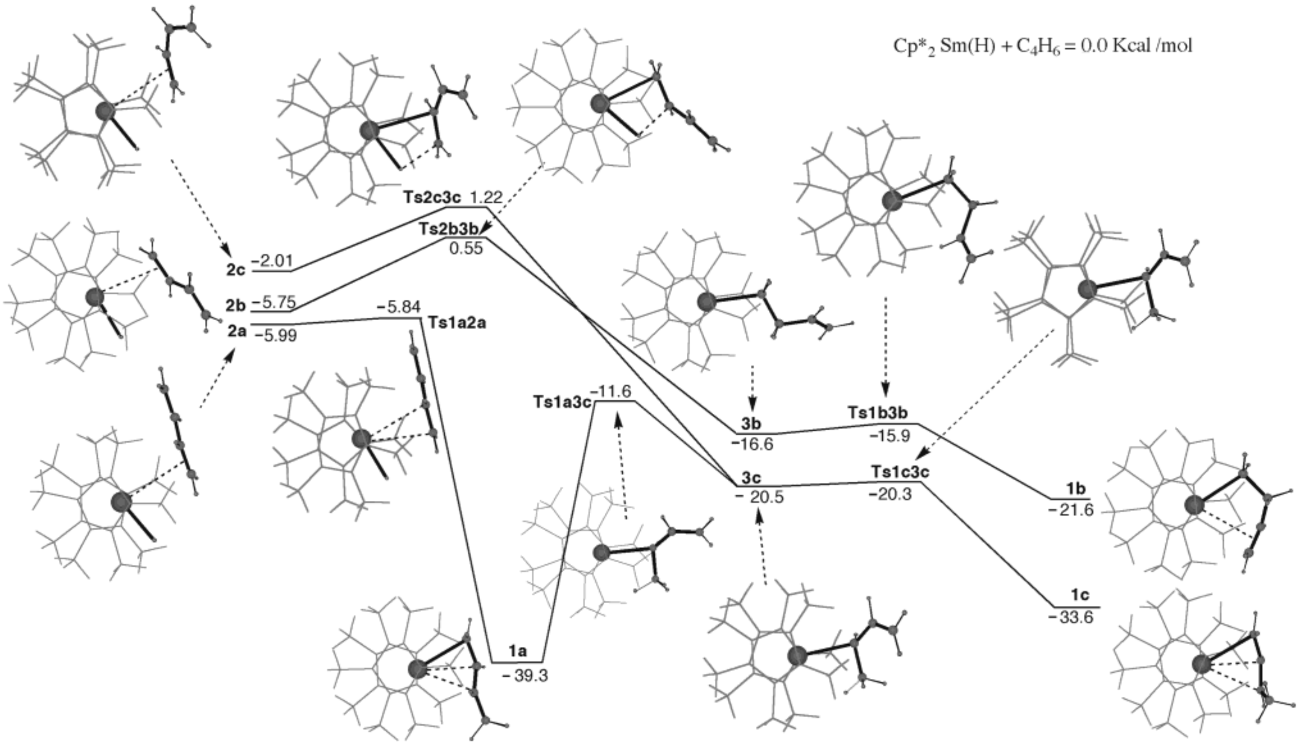

summarized in Chart 1 with their relative energies. Of the three metal−carbon bonds in the two $\pi$-allyl type isomers **1a** and **1c**, Sm−C(terminal) is the shortest (2.638 Å in **1a**, 2.676 Å in **1c**) and Sm−C(−Me) is the longest (2.803 Å in **1a**, 2.887 Å in **1c**) apparently due to the steric repulsion between the methyl group and those of the Cp* ligand, which is more pronounced in **1c** than in **1a**. In accord with larger steric repulsion in the *anti*-$\pi$-allyl complex, **1c** is 5.7 kcal/mol less stable than **1a** (Chart 1). As expected, complex **1b**, with the unconjugated but chelated butenyl ligand, is the least stable of the three, and its energy level lies 12 kcal/mol above that of **1c**.

**(3) Coordination of Butadiene.** All efforts to obtain a stationary state that represents $\eta^4$-coordination of butadiene to the Cp*$_2$Sm(H) moiety have not been successful, while an $\eta^2$-coordinated butadiene could easily be located. $\eta^2$-Coordination to Cp*$_2$Sm(H) gives rise to four isomers, arising from *cis*- and *trans*-conformations of butadiene itself and also *exo*- and *endo*-orientations of the free vinyl group with respect to the wedge-shaped metallocene unit. The structures of all four isomeric complexes were calculated by the RHF calculations first, but only three of these were refined by the B3LYP geometry optimizations as shown in Figure 2, because both *cis*- and *trans*-isomers with an *endo*-free vinyl group should give similar insertion products that are not important in the present study. Figure 2 shows, therefore, side views for two $\eta^2$-coordinated *trans*-butadiene complexes with *exo*- (**2a**) and *endo*-free vinyl groups (**2b**), together with a *cis*-butadiene complex with an *exo*-vinyl group (**2c**).

The *trans*-butadiene unit remains planar on coordination, while the *cis*-form in **2c** has the uncoordinated vinyl group twisted by ca. 30° from planarity. These structural features are the same as those observed in free *cis*-butadiene, suggesting that the *cis*-butadiene unit in **2c** is not deforming very much from its free state. However, due to steric repulsion between uncoordinated vinyl group and one of the Cp* ligands, the Sm−(−CH=) distance of 3.559 Å in **2c** is significantly larger than the corresponding bonds in **2a** (3.417 Å) and **2b** (3.356 Å), while the bond lengths of metal to the coordinated terminal carbons, Sm−(CH$_2$=), are similar in all cases. Since free *cis*-butadiene is 3.6 kcal/mol higher in energy than the free *trans*-form and **2c** is less stable than the *trans*-analogues by a similar amount, the steric congestion in **2c** makes only a slight contribution to its higher potential energy (Chart 1). Within *trans*-coordinated isomers, **2a** was calculated to be slightly more stable than **2b** (0.23 kcal/mol).

Having established coordination of butadiene (reactants), we next followed insertion reaction paths that should lead eventually to complexes with an $\eta^3$-butenyl unit of different conformations (products) already depicted in Figure 1.

**(4) Insertion Products with an $\eta^1$-Butenyl Ligand.** The migrative insertion reaction between Sm−H and the coordinated CC double bond should yield either an $\eta^1$-butenyl or $\eta^3$-butenyl complex depending on whether the vinyl group in the initially formed $\eta^1$-butenyl intermediate remains uncoordinated or can spontaneously coordinate to the metal center. Butadiene complex **2a** gives an $\eta^3$-butenyl complex (vide infra), but **2b** and **2c** were found to give $\eta^1$-butenyl intermediates **3b** and **3c**, respectively, structures of which are illustrated in Figure 3 (side view) and Chart 1 (top view). Sterically, **3c** is more crowded, the metal-bound carbon being secondary whereas it is primary in the case of **3b**. This is reflected in a little longer metal carbon bond in **3c** as compared to **3b** (2.538 vs 2.512 Å). Energetically, however, **3c** is more stable than **3b** by 4.4 kcal/mol (Chart 1) and may be explained by delocalization effect. The Sm−Me bond of Cp$_2$Sm(Me) was analyzed by Koga

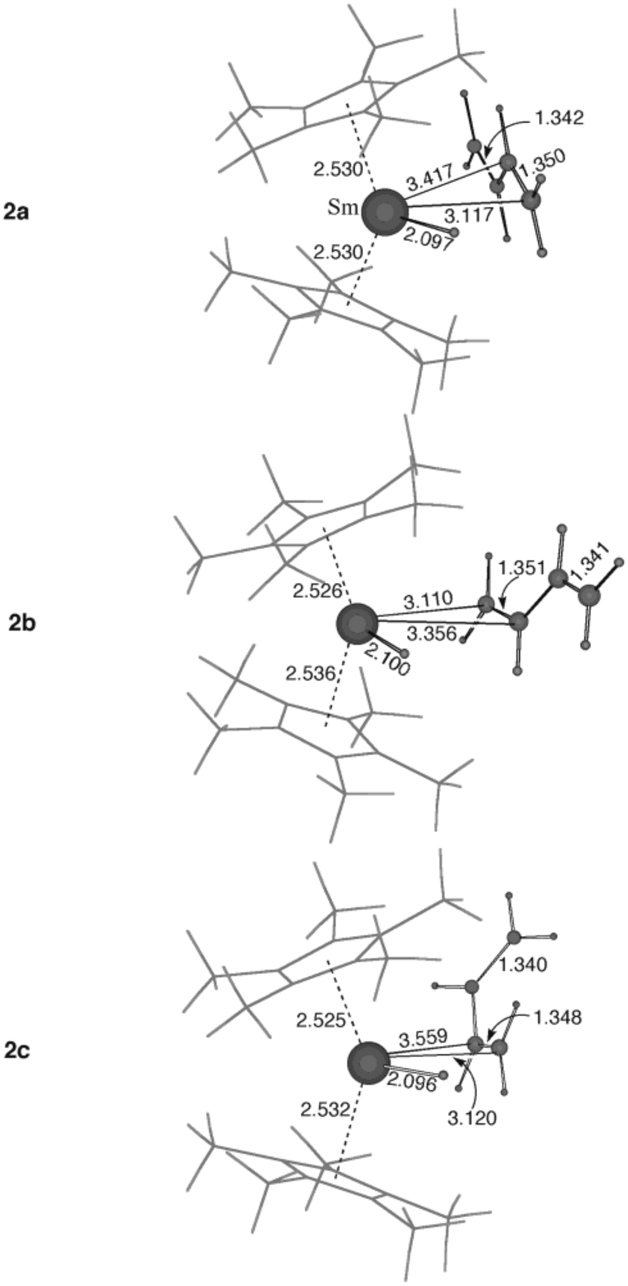

**Figure 2.** Computed geometries (Å) of Cp*$_2$Sm(H)(1,3-butadiene): **2a**, *trans*-butadiene with *exo*-oriented free vinyl; **2b**, *trans*-butadiene with *endo*-oriented free vinyl; **2c**, *cis*-butadiene with *exo*-oriented free vinyl.

to have significant ionic character, with a negative charge of −0.75 on carbon and a positive charge of +2.12 on Sm, which apparently is ascribed to the large difference in electronegativity between the two.[5a] It is not surprising that **3c**, whose free vinyl group is directly bound to a negatively charged carbon, has a lower total energy than **3b**. As a result of the delocalization, the uncoordinated C═C bond of **3c** (1.350 Å) is longer than that of **3b** (1.335 Å), while the formal single C−C bond of the former (1.467 Å) is shorter than the corresponding bond of the latter (1.508 Å).

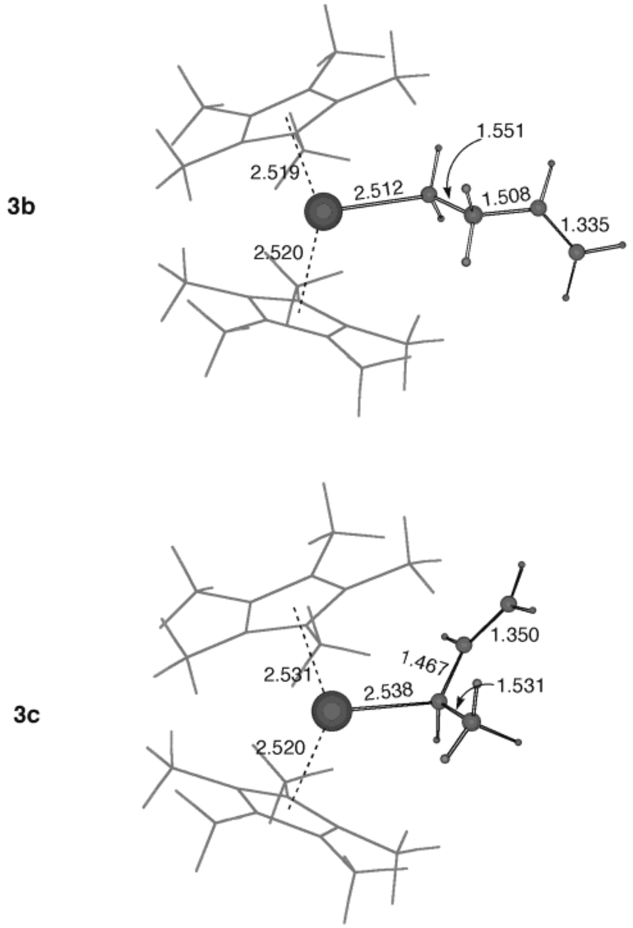

**Figure 3.** Geometries (Å) of insertion products with an $\eta^1$-coordinated butenyl group, **3b** and **3c**, derived from **2b** and from **2c**, respectively.

The geometries of the transition states **Ts2b3b** (transition state that connects **2b** and **3b**) and **Ts2c3c** (connecting **2c** and **3c**) are shown in Figure 4. They have a four-centered planar structure consisting of Sm−H and C═C, a typical geometry for a transition state that represents the middle stage of a migrative insertion process. However, reflecting the larger steric effect in **Ts2c3c**, its Sm−C($\sigma$) and H- -C bonds of 2.869 and 1.982 Å are significantly longer than those in **Ts2b3b**, 2.682 and 1.839 Å. Compared to their starting $\pi$-coordinated butadiene complexes, **Ts2b3b** and **Ts2c3c** are higher in energy by 6.30 and 3.23 kcal/mol, respectively.

**(5) Insertion Products with an $\eta^3$-Butenyl Ligand.** Obviously, the $\eta^1$-butenyl complexes **3b** and **3c** discussed in the preceding section give $\eta^3$-butenyl complexes **1b** and **1c** shown in Figure 1, simply by coordination of their vinyl group.

Transition states **Ts1b3b** and **Ts1c3c**, which connect **3b** and **1b**, and also **3c** and **1c**, are shown in Figure 5. The small uphill path (0.7 kcal/mol, Chart 1) from **3b** to **Ts1b3b** is the rotation of the −CH$_2$−CH$_2$− bond of the butenyl unit, but the terminal CC double bond is not yet interacting with the metal, as is obvious from the top view of **Ts1b3b** illustrated in Chart 1 and the long Sm−C(vinyl terminal) distance of 4.176 Å. Rotation of the vinyl unit, then, directs its $\pi$-orbitals to the central metal forming **1b**.

More important is the interconversion between **1c** and **3c**, being directly related to *anti*−*syn* interchange of substituted allyl ligands, a step that influences the specificity of *cis*- or *trans*-regulated 1,4-polymerization of butadiene.[4] Comparing the side view of **3c** (Figure 3)

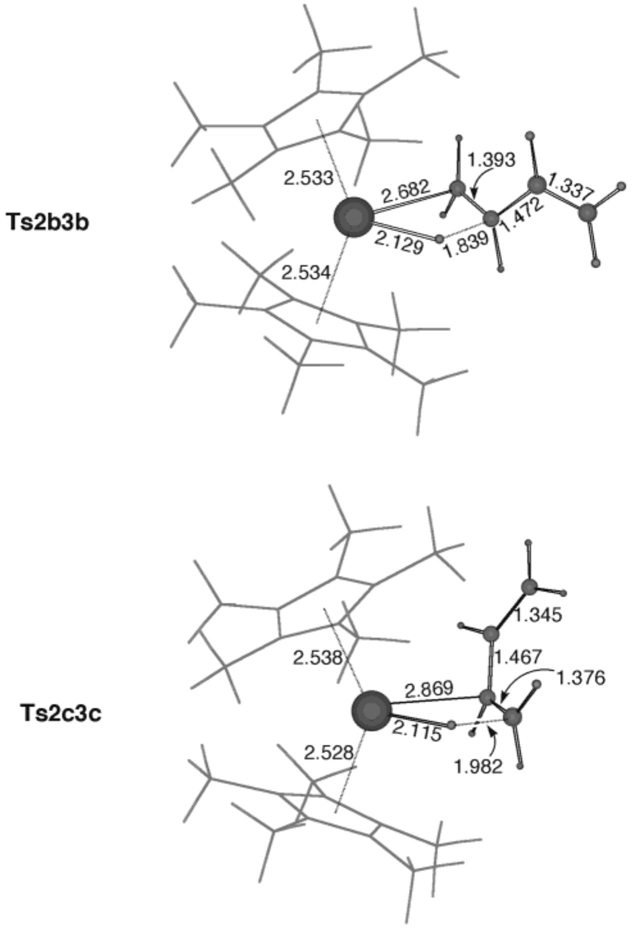

**Figure 4.** Computed geometries (Å) of transition states **Ts2b3b** and **Ts2c3c**.

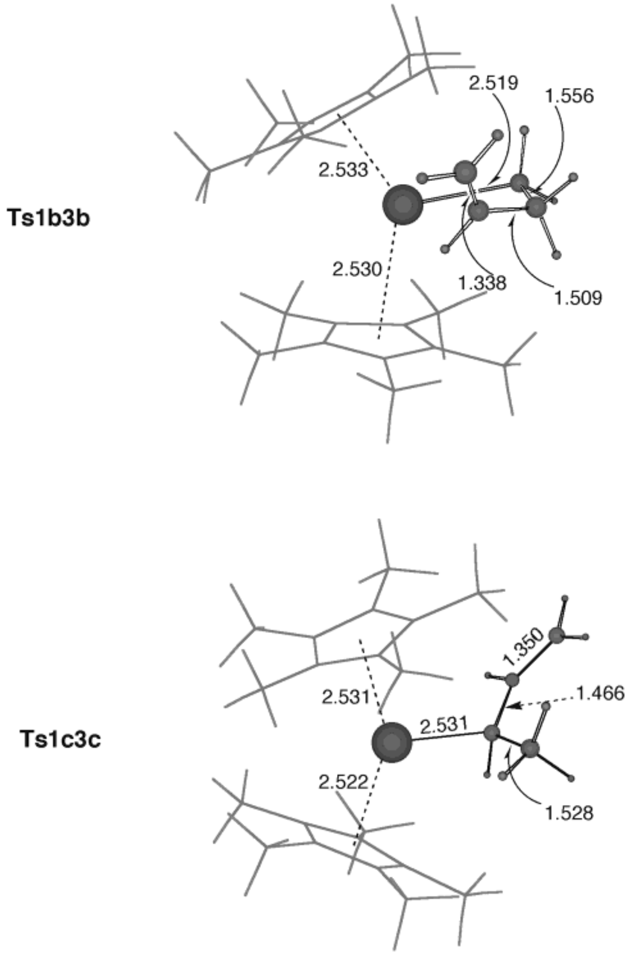

**Figure 5.** Computed structures (Å) of transition states **Ts1b3b** and **Ts1c3c**.

and **Ts1c3c** (Figure 5), one notices that the conformation of the butenyl unit stays very similar, while their top views (Chart 1) indicate that the relative orientation of the two Cp* rings has changed from staggered to eclipsed form. A very small energy difference of 0.2 kcal/mol is attributed to such rotational motion of the Cp* ligands, which provides space for the easier coordination of the CC double bond to the metal center. The formation of **1c** is attained mainly by rotating the Sm−C $\sigma$ bond of **Ts1c3c** anticlockwise with respect to the metal to carbon vector.

The *syn*-isomer **1a** is formed from the hydride−butadiene complex **2a** over a slight barrier of 0.15 kcal/mol (Chart 1). The zero-point correction made this value even smaller, 0.14 kcal/mol. This transition state **Ts1a2a** is located at a very early stage of the reaction, and its geometry is almost similar to that of **2a** (cf. Figures 2 and 6), the most noticeable change being a slight shift of the *trans*-butadiene unit toward the hydride on going to the transition state: (Sm)H−C(inserting vinyl terminal) distances is 3.158 Å in **2a** and 2.888 Å in **Ts1a2a**. The transition vector of the uncoordinated double bond (C3, C4) is directed toward the metal, while that of the coordinated terminal carbon (C1) is away from the metal. The vector of the hydride is toward C1, suggesting the migratory motion.

Relaxation of this transition state smoothly gives **1a**. Midway through that process, the complex was found to adopt an expected structure, shown below. The four-centered Sm−H−C1−C2 cyclic conformation is a counterpart of a similar local structure found in **Ts2c3c**. In

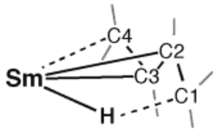

the present case, however, this structure is stabilized considerably by concomitant interaction of the adjacent double bond, C3−C4, with the metal, and hence this structure cannot be a transition state.

Another route to **1a** is to start from **3c** via transition state **Ts1a3c** (Chart 1), the geometry of which is depicted in Figure 6. The uphill change of **3c** to **Ts1a3c** is brought about by rotation of the central CC single bond, or rotation of the vinyl group, of **3c** by 67.5°. Further rotation of this bond induces interaction of the CC double bond with the metal, leading to the downhill process that readily gives **1a**. The conversion of **1a** to **1c**, the process of *syn*→*anti* isomerization, thus takes place via the highest point, **Ts1a3c**. Since the energy level of this transition state is rather high, 27.7 kcal/mol higher than that of **1a**, it is unlikely that the *syn*-isomer **1a** readily formed from **2a** further undergoes isomerization to the *anti*-form **1c** under normal conditions.

**(6) Rotation of the Coordinated Butenyl Unit.** In their investigation on fluxional behavior of *ansa*-

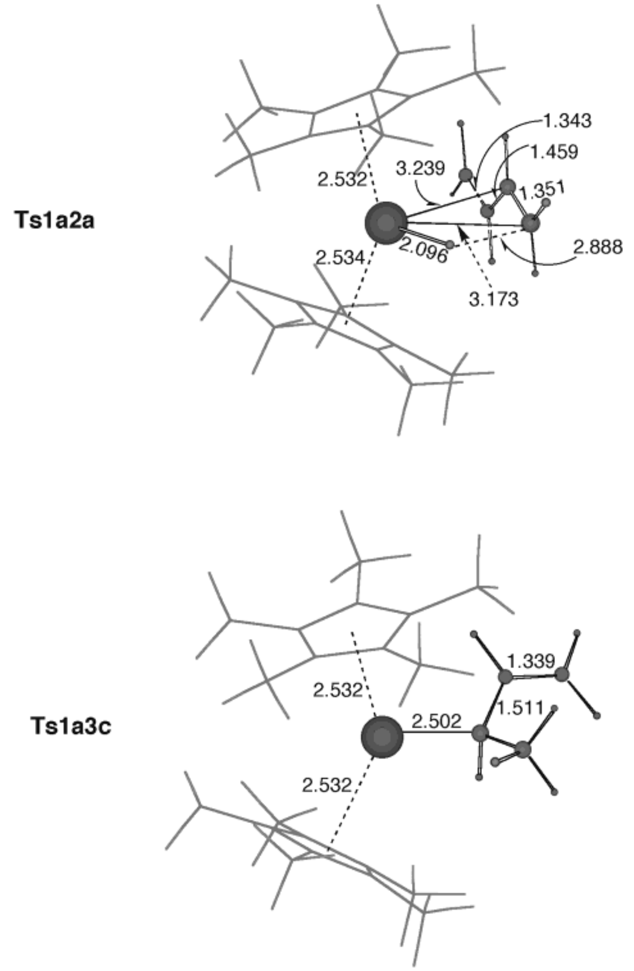

**Figure 6.** Computed structures (Å) of transition states **Ts1a2a** and **Ts1a3c**.

scandocene–$\eta^3$-allyl complexes, Bercaw et al. noted that the rate of $\eta^3$-allyl rotation is generally more than 1 order of magnitude faster than CC double bond dissociation from the metal center, i.e., $\eta^3$ to $\eta^1$ change in coordination.[11] The search for a stationary state that represents the rotational motion of the $\eta^3$-butenyl unit in **1a**, C1–C2–C3–Me, by starting the calculation from a geometry that restricts the C1–C3 vector of the $\eta^3$-allylic unit parallel to a metal–Cp*(centroid) vector, led to structure **1a′** shown in Figure 7. Complex **1a′** is an $\eta^1$-butenyl complex rather than $\eta^3$ and different from **3c** or **Ts1a3c** in that the terminal carbon is bonded to the metal center. It thus suggests that dissociation of the double bond from the metal takes place during the rotational process of the $\eta^3$-butenyl unit. By rotating the metal–carbon bond in **1a′** to either direction, $\eta^3$-coordination will easily be resumed and the energy difference between **1a** and **1a′** (14.7 kcal/mol) may be taken as the estimated rotational barrier of the $\eta^3$-butenyl unit.

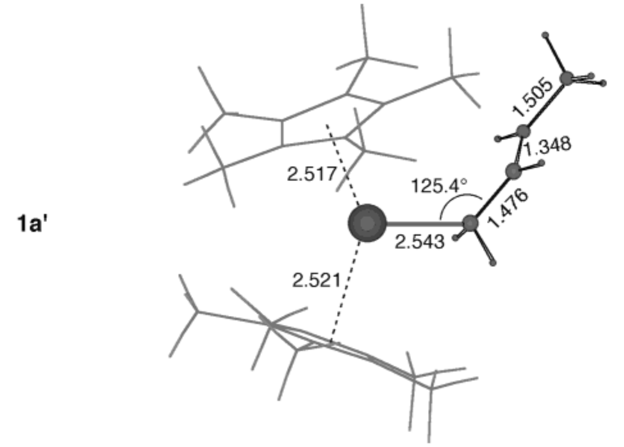

**Figure 7.** Computed geometry (Å) of the intermediate complex **1a′** relevant to allylic unit rotation in **1a**.

The haptotropic change **1a** → **1a′** is a process that opens a coordination site available to other reactant molecules: a closely related complex $[Cp^*_2Sm(\mu\text{-}\eta^3\text{-}CH_2CHCH_2\text{-})]_2$ (**4**) has been reported to initiate polymerization of ethylene presumably by adopting an $\eta^1$-coordination similar to the butenyl unit in **1a′** and thereby accepting an incoming ethylene molecule.[1] We found that complex **4** can also induce polymerization of butadiene at elevated temperatures. When heated to 100 °C with 500 equiv of butadiene for 4 h, polybutadiene with a sharp molecular weight distribution ($M_w/M_n = 1.69$, $M_w = 29\,000$) was obtained in 10% yield. As expected from the potential surface shown in Chart 1, the polymer was *trans*-rich. Detailed analysis and exploration of this and related polymerization systems are under investigation.

**Acknowledgment.** Financial support of this work by RIKEN through the Eco-molecular Science Program is gratefully acknowledged. We also thank the RIKEN Computer and Information Division for providing the computational facilities.

**Supporting Information Available:** Cartesian coordinates for all optimized structures at the B3LYP level, their absolute total energy values, and the imaginary frequencies for the transition state structures.

OM030162E

---

(11) Abrams, M. B.; Yoder, J. C.; Loeber, C.; Day, M. W.; Bercaw, J. E. *Organometallics* **1999**, *18*, 1389.